View Article Online / Journal Homepage / Table of Contents for this issue

PCCP
Physical Chemistry Chemical Physics

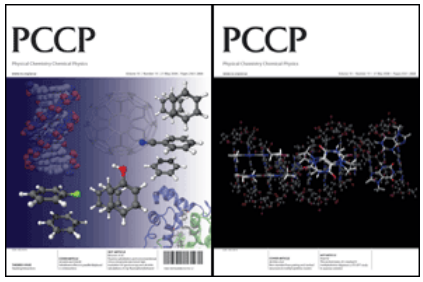

This paper is published as part of a PCCP Themed Issue on:

Stacking Interactions

Guest Editor: Pavel Hobza

Published on 21 February 2008. Downloaded by Michigan State University on 23/01/2016 03:22:09.

Editorial

Perspectives

Papers

View Article Online

Published on 21 February 2008. Downloaded by Michigan State University on 23/01/2016 03:22:09.

N–H···π interactions in pyrroles: systematic trends from the vibrational spectroscopy of clusters†

Ingo Dauster, Corey A. Rice, Philipp Zielke and Martin A. Suhm*

Received 19th November 2007, Accepted 15th January 2008
First published as an Advance Article on the web 21st February 2008
DOI: 10.1039/b717823a

Published on 21 February 2008. Downloaded by Michigan State University on 23/01/2016 03:22:09.

Pyrrole and some of its methylated derivatives are aggregated in a controlled way in pulsed supersonic jet expansions. The cluster N–H stretching dynamics is studied using FTIR and Raman spectroscopy. Dimers, trimers and tetramers can be differentiated. Systematic trends in the dimer N–H···π interaction as a function of methyl substitution are identified and explored for predictions. Overtone jet absorption spectroscopy is used to extract anharmonicities for the N–H bond in different environments. The N–H anharmonicity constant increases by 10% upon dimerization. Bulk matrix shifts can be emulated by the formation of Ar-decorated clusters. The experimental results are expected to serve as benchmarks for an accurate *ab initio* characterization of the N–H···π hydrogen bond.

1. Introduction

There is an intermediate hydrogen-bond regime[1,2] between classical hydrogen bonds such as O–H···O[3] or aromatic N–H···N[4] contacts on one side and very weak, unspecific interactions involving hydrogen bridges such as C–H···F[5,6] on the other. Such secondary intermolecular contacts are believed to play a pivotal role in molecular-recognition phenomena, while stronger attractions are typically responsible for intermolecular cohesion. In aqueous solution, where classical hydrogen bonds within the solute compete with classical hydrogen bonds to the solvent, the intermediate hydrogen bonds may have structural effects which are comparable to the net effect of strong hydrogen bonding. It is thus rewarding to study model systems involving interactions of such intermediate strength.

The intermolecular interaction of sp^2-hybridized N–H groups with the charge density of π systems falls in the upper range of this regime. It is an important contact in biomolecular systems.[7] Pyrrole (C_4H_4NH) is one of the simplest, biologically most abundant and most versatile model systems which allows for its study. It provides compact donor and acceptor groups combined in one molecule which leads to characteristic self-aggregation phenomena. Pyrrole may serve as an elementary prototype for the experimentally more accessible indole[8] system and its biological derivatives. It is used in supramolecular design,[9] recently even claiming nanoparticle morphology control.[10] A perpendicular arrangement of two pyrrole planes does not allow for symmetric binding in the dimer nor for π-stacking interactions. Therefore, the pyrrole dimer assumes a compromise geometry[11] with an inter-plane angle of 55°. Larger clusters provide avenues for cooperativity, because they allow for a cyclic hydrogen-bond topology, much like that of hydrogen fluoride[12] or alcohol clusters.[13]

Pyrrole and its derivatives have been studied extensively using different spectroscopic techniques,[14,15] but intermolecular interaction has rarely been at the focus of such investigations.[16] Available cluster studies have typically concentrated on the pyrrole dimer.[11,17] Notable exceptions are a detailed matrix isolation study[18] and a recent photochemical molecular-beam investigation.[19] While electronically excited states of pyrrole exhibit biologically relevant dynamical properties,[19,20] the present contribution will focus exclusively on the electronic ground state of pyrrole and its clusters. The literature on the pyrrole monomer has been summarized comprehensively in ref. 18 and shall not be repeated here in detail. We note that a previous infrared supersonic jet study[15] observed mass-spectrometric evidence for dimers but concentrated on the spectroscopy of the monomer. An infrared study of the isolated pyrrole dimer and larger clusters therefore appeared timely. After submission of the present manuscript, we learned about an independent IR cavity ringdown study of small and large pyrrole clusters in the N–H stretching range which has now appeared in print.[21] Wherever there is overlap between the two contributions, the agreement is excellent and we refer to it in the following. Furthermore, there is a very recent study of size-selected pyrrole clusters[22] which concentrates on their fragmentation upon ionization.

The pyrrole dimer may be viewed as a complex which involves significant dipole–dipole attraction and dispersion interactions, as well as a perpendicular N–H···π bond tendency. The angle between the two pyrrole planes is fairly small (55°)[11] and reflects this competition between parallel dipole–dipole and π-stacking preferences and the more orthogonal hydrogen-bond preference. Intermolecular interaction affects the vibrational dynamics of the monomers, in particular in the N–H stretching and low-frequency C–H/N–H out-of-plane bending modes.[18] Since the N–H stretching mode is more accessible to supersonic jet studies, we concentrate on its dynamics in this work. The vibrational dynamics of

Institut für Physikalische Chemie, Universität Göttingen, Tammannstr. 6, 37077 Göttingen, Germany. E-mail: msuhm@gwdg.de
† The HTML version of this article has been enhanced with colour images.

Published on 21 February 2008. Downloaded by Michigan State University on 23/01/2016 03:22:09.

methylated pyrrole derivatives has been studied less frequently.[23] In the present study, it serves the purpose of fine-tuning the hydrogen-bond interaction.

For practical reasons, most of the previous self-aggregation studies of pyrrole have been carried out in solvents.[16,17] However, the CCl_4 solvent shift of the N–H stretching vibration amounts to 40% of the dimerization shift, making it somewhat questionable whether hydrogen-bond-induced frequency shifts in solution can be interpreted reliably. The weaker and the less directional a hydrogen bond is, the more important it is to extend its study into the gas phase. Only in this way can one ensure that the interaction is not dominated by packing or solvent forces.[2,17]

To enable a proper comparison between theory and experiment in the field of hydrogen-bond frequency shifts, it is imperative to understand the influence of hydrogen bonding on anharmonicity.[24] The present work also contributes to this issue by reporting some of the first overtone absorption spectra of jet-cooled organic hydrogen-bonded clusters.[25]

2. Experiment

The FTIR spectra (Bruker Equinox 55, 2 cm^{-1} resolution) have been obtained by synchronization with buffered gas pulses[12,13] emerging from a 600-mm-long slit nozzle (filet jet[26]), which are controlled by a series of six magnetic values. Pulsed jet experiments need to be more sophisticated[27–29] for high-resolution FTIR studies,[30] but are straightforward and very helpful for the present low- to medium-resolution cluster spectroscopy.[13] The gas consists largely of helium (99.996%) or argon (99.998%) with a variable trace admixture of one or two pyrrole derivatives. The mixing ratio is controlled by adjusting the temperatures of two thermostatted saturators containing the liquid or solid compounds through which the rare gas flows. Suitable optical band-pass filters are employed to improve the spectral quality in selected regions. To detect infrared-inactive bands in cyclic clusters, Raman jet spectroscopy[31] was also applied in the case of pyrrole. A 4 mm slit nozzle fed by a single magnetic valve was employed and combined with a 5 W laser (Coherent), a 1000 mm monochromator (McPherson 2051) and a 1024 × 128 pixel CCD camera (Andor DV401-FI).[32] The spectra were calibrated to Ne lines with an estimated wavenumber accuracy of 1–2 cm^{-1}. Some Raman spectra revealed an unusual frequency-independent scattering background which we attribute to progressive pyrrole polymerization in the liquid sample, giving rise to polymer aerosol formation. The size of the aerosol was estimated to be in the μm range, but its effect was easily removed by shifting the baseline of the scattering spectra.

By varying the stagnation pressure or concentration of the expansions, signals from different cluster sizes can be distinguished. The distance from the nozzle has a strong influence on the effective vibrational and rotational temperature of the clusters. In the Raman experiment, it was necessary to probe as close as 1 mm from the nozzle, whereas the FTIR experiment probed the expansion at a distance of 10 ± 10 mm.

Gas-phase and liquid-state reference spectra for pyrrole have been recorded in the jet chamber and in a ZnSe attenuated total reflection (ATR) cell at room temperature respectively. Pyrrole (Aldrich, 98%; Acros, 99%; ABCR 98%), 1-methylpyrrole (Lancaster, 99%), 2,5-dimethylpyrrole (Aldrich, 98%), 1,2,5-trimethylpyrrole (Aldrich, 99%) and benzene (Acros, 99%) were used as supplied.

In order to obtain theoretical Raman intensities, some of the quantum-chemical calculations available in the literature[18] (B3LYP/6-311++G(d,p), in short B3LYP) were repeated and extended to the PW91/PW91 functional with the 6-311++G(d,p) basis set (in short PW91) using the Gaussian 03 program suite.[33] Slight differences in B3LYP harmonic wavenumbers compared to those reported previously[18] may be accounted for by the use of symmetry in combination with the finite integration grids. No counterpoise correction was applied to the binding energies and the quality of the calculations should not be overestimated in view of significant dispersion contributions in such systems.

3. Results and discussion

3.1 Self-aggregation of pyrrole

Fig. 1 shows the N–H stretching FTIR spectrum of 0.04% pyrrole expanded in He at increasing stagnation pressures (center part). For comparison, the top segment contains a room-temperature gas-phase spectrum without clusters and a room-temperature liquid-phase spectrum which indicates the expected range of N–H frequency shifts due to hydrogen bonding. The spectral separation and successive appearance of the individual bands marked M, D, T in these and other jet spectra with increasing pressure clearly indicates a progressive cluster size because cooperativity increases with size and the decreasing hydrogen-bond strain in cyclic clusters assists this trend. Based on many related studies, one can safely assume that the bands correspond to pyrrole monomer[14] (fundamental M, hot band M_{hb}), dimer donor (D_d) and trimer (T). The wavenumbers obtained are also in excellent agreement with those recently reported in a cavity ringdown study.[21] Only one strongly IR-active band is found for the trimer. This implies a cyclic (C_{3h}) structure (shown as a cartoon in Fig. 1). Still further red-shifted, there is a weak band at high stagnation pressure which we attribute to pyrrole tetramer (Te, see top trace of Fig. 2) in a cyclic C_{4h} structure[18] with a degenerate IR-active band.

In the case of the dimer, an open (C_s) structure with a free N–H band overlapping with the monomer absorption is more likely. The Raman jet spectrum (second-lowest trace in Fig. 1) confirms that this is indeed the case, fully in line with previous microwave evidence.[11] The weak shoulder on the low-frequency IR band slope of the monomer turns out to be the missing dimer acceptor band (D_a), which is better resolved in the colder slit-jet IR cavity ringdown spectra.[21] Two reasons account for its even better visibility in the Raman spectrum. The N–H stretching band profiles are dominated by Q-branch transitions and are therefore an order of magnitude more narrow than the IR transitions despite the lower rotational temperature of <20 K in the IR experiment. Furthermore, the dimer donor and dimer acceptor bands have comparable intensities in the Raman spectrum, whereas the acceptor band lacks the strong IR intensity enhancement of the donor band

 This journal is © the Owner Societies 2008

Published on 21 February 2008. Downloaded by Michigan State University on 23/01/2016 03:22:09.

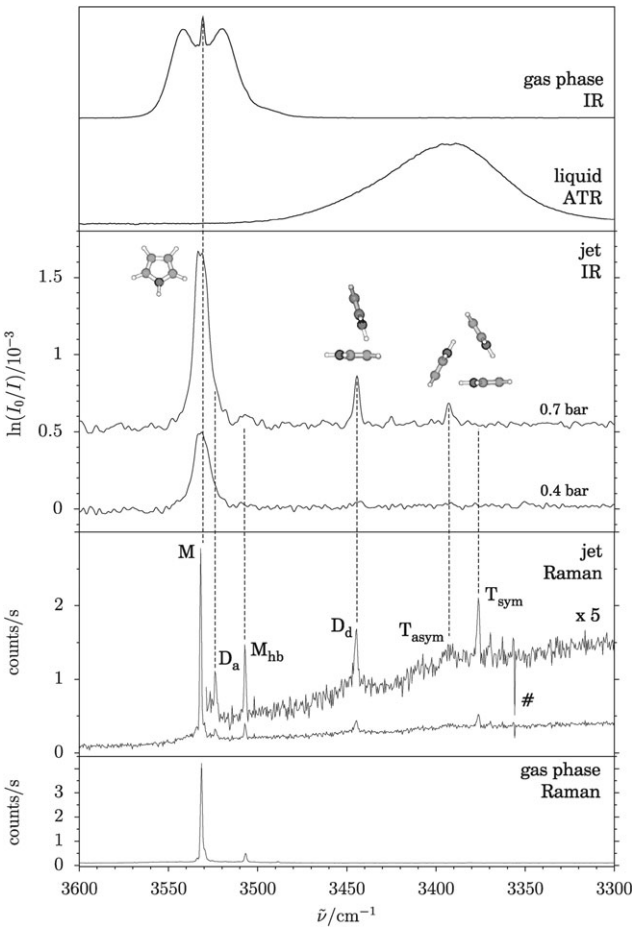

Fig. 1 IR and Raman spectra of the N–H stretching fundamental of pyrrole in different aggregation states. The top segment shows room-temperature gas-phase absorption and liquid-state attenuated-reflection spectra which span the aggregation shift. The central segment shows jet FTIR spectra recorded at different stagnation pressures (0.04% pyrrole in He, 200 scans each) together with monomer, dimer and trimer structures. The bottom segment shows gas-phase and jet Raman spectra. # marks a CCD camera artifact. See text for details.

and is therefore hidden in the slope of the dominant monomer signal. Another feature (marked M_{hb}) visible in both the IR and Raman spectra has a monomer origin, as evidenced by the dimer-free Raman gas-phase spectrum (bottom trace) and as discussed earlier.[14] It corresponds to a hot transition originating in the low frequency out-of-plane bending vibration state (ν_{16} at 474.61 cm^{-1}). The M : M_{hb} Raman intensity ratio in the gas phase and in the jet can be used to estimate the amount of vibrational cooling of the ν_{16} vibration in the jet. The intensity depletion in the jet corresponds to only $\approx$10 K of cooling. This is in contrast to the rotational cooling which is more than an order of magnitude stronger even 1 mm ($\approx$7 slit widths) away from the nozzle, based on investigations of other molecules. It is well known that vibrations, and in particular the lowest vibrations of a molecule, may cool inefficiently in a supersonic jet spectrum. However, this does not affect the applicability of supersonic jets in the investigation of clusters. Furthermore, the vibrational cooling in the FTIR jet spectrum, which is recorded up to 100 nozzle diameters downstream, is significantly higher. It can be estimated at $\approx$100 K below the nozzle temperature from the corresponding hot-band intensity, also using the room-temperature gas-phase intensity ratio[14] as a reference. Rotationally colder spectra of pyrrole and its clusters have recently been obtained in a pinhole expansion.[21]

Therefore, the Raman and IR spectra of the pyrrole dimer are fully consistent with each other. The acceptor band is shifted by about 7 cm^{-1} to a lower wavenumber compared to the monomer band center. The harmonic PW91 (B3LYP) prediction is 6 cm^{-1} (5 cm^{-1}) in the same direction. This shift results from the softening of the N–H bond upon pyrrole acting as a hydrogen-bond acceptor. The donor band is shifted in the same direction by 86 cm^{-1} (87 cm^{-1} from the Raman spectrum). At the harmonic PW91 level, this shift is overestimated by about 25%, whereas it is underestimated by about 17% at B3LYP level. In line with many other hydrogen-bonded systems, the red-shift is more pronounced for the donor mode than for the acceptor mode. That is largely due to a smaller intramolecular force constant in the bridging N–H.[3] Indeed, the effect is close to that of classical hydrogen bonds (*e.g.* 111 cm^{-1} for the methanol dimer[34] or about 135 cm^{-1} predicted for pyrrole–water[35]). This suggests that the N–H$\cdots\pi$ interaction in the pyrrole dimer comes quite close to a classical hydrogen-bond interaction. Even more so if one considers that for a given binding energy the N–H oscillator is less susceptible to red-shifts than the O–H oscillator, at least in solution.[36] Quantum-chemical calculations indeed support a substantial binding energy of the dimer between 12 and 21 kJ mol^{-1},[18,37] whereas the dimer-stretching force-constant estimated from centrifugal-distortion data indicates a significantly weaker interaction.[11] Here, higher-level benchmark calculations would be desirable. A recent counterpoise-corrected MP2 calculation[22] yields 23 kJ mol^{-1}, but may have to be extended to larger basis sets. The experimental intensity ratio between the acceptor and donor bands can only be estimated very approximately around 1 : 10–1 : 5 in the IR case. This is in line with the harmonic PW91 (B3LYP) prediction of 1 : 6 (1 : 4). In the experimental Raman spectrum, the acceptor : donor ratio is between 1 : 2 and 2 : 3 (PW91, 1 : 4; B3LYP, 1 : 3).

The trimer is predicted to have C_{3h} symmetry,[18] with every molecule acting simultaneously as a donor and as an acceptor (see Fig. 1). This leads to a degenerate (E') IR-active stretching vibration, which corresponds to an out-of-phase motion of the N–H bonds. The in-phase (A') transition is IR-forbidden by symmetry but strongly Raman-allowed, like in the phenol trimer case.[38] This is confirmed in the experimental spectra. The strong IR band (T_{asym}) corresponds to a weak and broad Raman band which lacks a pronounced Q-branch due to the E' symmetry-selection rules. To lower wavenumber, an exclusively Raman-active band with a prominent Q-branch is observed (T_{sym}). The splitting between the two bands, 17 cm^{-1}, is called a Davydov splitting and represents a sensitive measure for the N–H oscillator coupling across the hydrogen bond. In the present case, it means that the three equivalent N–H stretching modes in the trimer are in resonance—either through space or *via* their influence on the acceptor π-system—and their degeneracy is lifted. The coupling may

Published on 21 February 2008. Downloaded by Michigan State University on 23/01/2016 03:22:09.

be represented by a Hückel-like determinant, where x is the energy shift relative to the zeroth order energy and W is the coupling constant between monomer units:

$$\begin{vmatrix} x & W & W \\ W & x & W \\ W & W & x \end{vmatrix} = 0 \qquad (1)$$

The solutions are $x = -2W$, W, W. The coupling constant W[34] thus amounts to one third of the splitting, *i.e.* 6 cm^{-1} in the pyrrole trimer. For an indirect coupling mediated *via* a π-system this is a respectable magnitude, but direct couplings in aromatic and aliphatic alcohol trimers are larger.[34,38] Again, this confirms the sizeable strength of the pyrrole hydrogen bonds. A good-quality trimer force field is expected to reproduce this observed Davydov splitting reasonably well, at least upon inclusion of anharmonic effects. The corresponding analysis of methanol clusters[34] suggests that even the harmonic approximation might be acceptable in many cases. Indeed, an exploratory pyrrole-trimer calculation at the PW91 level predicts a Davydov splitting of 17 cm^{-1}. At the B3LYP/6-311++G(d,p) level,[18,21] the Davydov splitting amounts to 11–12 cm^{-1}.

The experimental red-shifts of the two trimer bands relative to the monomer (138 cm^{-1} for the E' mode, 155 cm^{-1} for the A' mode) are much larger than that of the dimer donor mode (86 cm^{-1}). The harmonic trimer red-shifts at PW91 level are 13–15% too large; the B3LYP predictions are 26% too small. The enhanced trimer red-shifts compared to the dimer reflect the cooperativity of the trimer hydrogen-bond pattern, despite some residual ring strain which may still be expected in the triangular arrangement. Based on the microwave structure of the dimer,[11] which involves an angle of 55° between the pyrrole planes, the ring strain cannot be very large as the C_{3h} symmetry implies an angle of 60°. However, the predicted dimer angle is quite different at the B3LYP (73°) and PW91 (70°) levels, indicating a deficiency of density functionals in describing the directionality of this moderately strong hydrogen bond. Energetically, the cooperativity is only moderate according to the PW91 (B3LYP) calculations. While the dimer is electronically bound by about 21 kJ mol^{-1} (14 kJ mol^{-1}), a hydrogen bond in the trimer contributes 23 kJ mol^{-1} (16 kJ mol^{-1}).

There is further experimental evidence that the ring strain in the pyrrole trimer must be less than in alcohol trimers. The IR spectrum in Fig. 2 (top trace) shows that the tetramer absorption (Te) is only shifted by another 10 cm^{-1} relative to the trimer. This is a small increment, considering that there will also be some cooperativity enhancement when moving from the trimer to the tetramer. For alcohol clusters, cooperativity and ring-strain effects between the trimer and the tetramer are much larger.[34] The tetramer concentration in the Raman spectrum is too low to allow for an unambiguous determination of the Davydov splitting among the four local oscillators.

At this stage, it is instructive to compare the isolated jet spectra reported here with the Ar matrix-isolation spectra obtained earlier.[18] The latter have tentatively been interpreted in terms of different cluster-size contributions to the aggregation bands, although the width of the bands makes a definitive assignment difficult. The comparison between bulk matrix

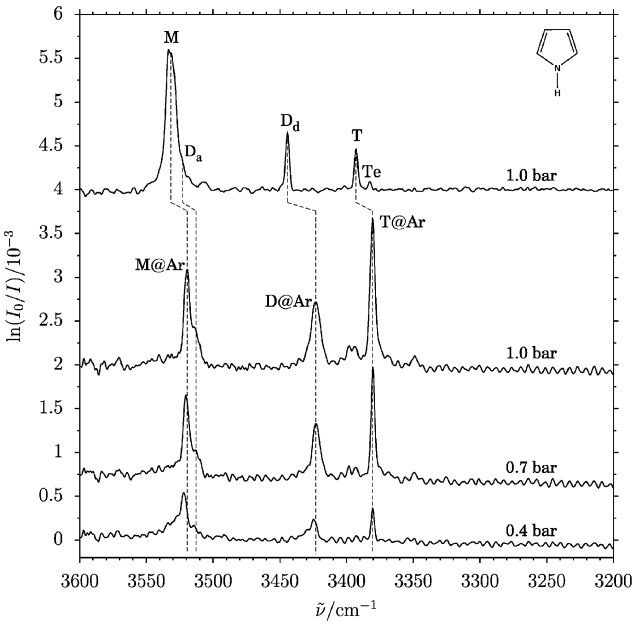

Fig. 2 Jet FTIR spectra (≈0.04% pyrrole, 200 scans each) of the N–H stretching fundamental of pyrrole and its clusters in He (top trace) and in Ar (next three traces with decreasing stagnation pressure). The latter correspond to Ar-decorated clusters.

isolation and vacuum isolation is made in Table 1. The Ar matrix shift of the monomer N–H stretching vibration is on the order of −10 cm^{-1}, quite a typical value for a hydride stretching mode interacting with argon. It is somewhat larger for the acceptor N–H in the dimer. The donor vibration is found to shift three times more than the monomer in a bulk Ar matrix. In part, this may be a packing effect which compresses the pyrrole dimer hydrogen bond. However, such shifts are not easy to rationalize in general.[39] Surprisingly, the IR-active N–H stretching band assigned to the pyrrole trimer in the Ar matrix[18] is blue-shifted with respect to the now available gas-phase value. It has been observed repeatedly that hydrogen-bonded trimers show unusually small red-shifts or even slight blue-shifts upon Ar-embedding.[13,28,39] Nevertheless, we consider it possible that the further red-shifted band tentatively assigned to tetramers in the matrix-isolation work[18] may actually be due to trimers. We provide this alternative assignment in Table 1 in square brackets.

To further elucidate the matrix effects, we have carried out supersonic jet expansions of pyrrole using Ar instead of He as the carrier gas. Fig. 2 shows the result as a function of stagnation pressure. The bands are now characteristically shifted with respect to their positions in a He expansion (top trace, see also Table 1). The shift is due to condensation of Ar atoms on the pyrrole monomers and clusters. There is a slight asymmetry in the low-pressure monomer and dimer spectra as well as a progression of the band maximum shift with increasing stagnation pressure, shown by the guiding lines. This reflects a progressive coating in particular of the monomer and dimer with increasing pressure.[40] However, the Ar is seen to condense on pyrrole and its clusters even at the lowest stagnation pressures employed. Recently, mixed pyrrole–Ar clusters have also been observed in a size-selected ionization

 This journal is © the Owner Societies 2008

Published on 21 February 2008. Downloaded by Michigan State University on 23/01/2016 03:22:09.

Table 1 Experimental wavenumbers ν_{NH}/cm^{-1} and corresponding Ar shifts and hydrogen-bond shifts for the pyrrole monomer (M), dimer (donor D_d, acceptor D_a) and trimer (T) from a supersonic jet expansion in He (isolated), in Ar (Ar-coated) and an Ar matrix isolation (Ar matrix[18]) study

Absolute wavenumbers			
System	Isolated	Ar-coated	Ar matrix[18]
M	3531 3530.8[14]	3519	3521–23
D_a	3524	3514	3510
D_d	3444	3423	3409–3418
T(*E*′)	3393	3381	3396 [3378]

Ar-induced shifts			
System	Isolated	Ar-coated	Ar matrix[18]
M	—	−12	−(8–10)
D_a	—	−10	−14
D_d	—	−21	−(27–36)
T(*E*′)	—	−12	+3 [−15]

Hydrogen bond shifts			
System	Isolated	Ar-coated	Ar matrix[18]
M	—	—	—
D_a	−7	−5	−(11–13)
D_d	−86	−96	−(105–112)
T(*E*′)	−138	−139	−(125–127) −[143–145]

study.[22] The bands in our nanomatrix-isolation experiment are far more structured than the aggregation bands in a bulk matrix,[18] due to a different formation mechanism. The nanomatrices are probably amorphous and adapt themselves to the molecular geometry, whereas the more-or-less crystalline bulk matrices involve stronger packing effects and site splittings. Due to the better size resolution, it is straightforward to assign the monomer (M@Ar), dimer acceptor and donor (D@Ar) and infrared-active trimer bands (T@Ar). The latter gains much in intensity due to the improved collisional cooling efficiency of Ar. The tetramer signal is hidden in the noise and possibly falls underneath the trimer signal. The corresponding Ar-coating shifts are also tabulated in Table 1 and behave more regularly. They indeed suggest a slight reassignment of the trimer band in the bulk argon matrix, but the width and structure of the latter makes a unique interpretation difficult.

The most straightforward comparison with theoretical N–H stretching wavenumber predictions is possible for the isolated clusters. To compensate for inaccuracies in the monomer description and in part also anharmonic effects, we restrict the discussion to wavenumber shifts upon complexation. The experimental shifts (−7 and −86 cm^{-1} for the dimer, −138 and −155 cm^{-1} for the trimer, −148 cm^{-1} for the tetramer) compare reasonably well to the unscaled B3LYP/6-311++G(d,p) results[18] (−5, −71; −102, −114; −120 cm^{-1} respectively). The theoretical predictions are systematically smaller than the experimental shifts. In normal hydrogen bonds, the opposite is often the case for hybrid density functionals. This may indicate that there are binding contributions in pyrrole clusters which are underestimated by the B3LYP functional. Such a conclusion would not be surprising given the deficiencies of DFT in the field of dispersion interactions. However, the variation among different density functionals is disappointingly large. Our exploratory PW91/6-311++G(d,p) calculations yield harmonic shifts which are typically larger than those observed experimentally (−6, −109 cm^{-1} for the dimer; −159, −175 cm^{-1} for the trimer). 50% differences such as these reduce the predictive power of density functional theory significantly. The present experimental results should thus encourage theoretical studies of N–H···π interactions at significantly higher levels of electron correlation.

In summary, the hydrogen-bond-induced red-shifts of the N–H stretching bands increase progressively with cluster size and an Ar surrounding increases in particular the dimer red-shift, which provides an indirect confirmation of its open structure, as compared to the clearly cyclic arrangement in the trimer. The latter is demonstrated beyond doubt by the combination of IR and Raman spectroscopy. Matrix shifts can be characterized in more detail by the study of Ar-coated monomer and clusters.

3.2 Experimental anharmonicity analysis of the pyrrole dimer

While the experimental and thus anharmonic pyrrole dimer shifts of −7 and −86 cm^{-1} can already serve as reasonable benchmarks for accurate harmonic calculations, it would be better to take anharmonicity effects into account explicitly. On the theoretical side, their inclusion can be quite challenging for a polyatomic system, in particular beyond an approximate perturbational level. If experiment provided truly harmonic shift values, the comparison would be much more straightforward. Within the local mode approximation for the N–H mode, the analysis of overtone transitions can yield such experimental harmonic values. Unfortunately, overtones of hydrogen-bonded hydride stretches are exceedingly weak.[25] In the present case, we were nevertheless able to observe them in the jet expansion for the dimer (Fig. 3), although they barely

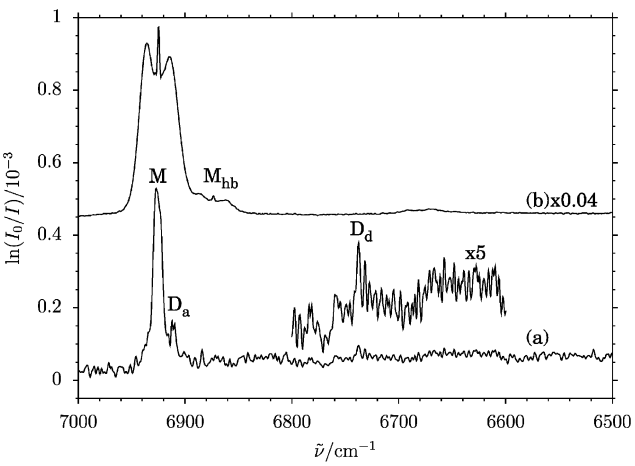

Fig. 3 Jet FTIR spectrum (1050 scans, ≈0.2% pyrrole) of the N–H stretching overtone of pyrrole and its clusters [bottom trace (a)] compared with the room-temperature gas-phase spectrum in He [top trace (b)]. The jet spectrum in the dimer region is also magnified by a factor of 5.

Published on 21 February 2008. Downloaded by Michigan State University on 23/01/2016 03:22:09.

Table 2 Experimental anharmonicity analysis for the pyrrole monomer (M) and dimer acceptor (D_a) and donor (D_d). All values are in cm^{-1}

System	$\tilde{\nu}_{N-H}$	$2\tilde{\nu}_{N-H}$	$\omega_e x_e$	ω_e	$\Delta\omega_e$
M	3531	6925	68.5	3668	
Ref. 14 and 42	3530.8	6924.6	68.5	3667.8	
D_a	3524	6911	68.5	3661	−7
D_d	3444	6738	75	3594	−74

rise above the noise level. It is noteworthy that the acceptor band is now stronger than the donor band, whereas the opposite is true for the fundamental range. This breakdown of hydrogen-bond-induced band-strength enhancement in the overtone range is a well-known consequence of the general shape of the dipole curve in hydrogen-bonded systems.[25,41] However, the present case is among the first direct proofs for a hydrogen-bonded hydride stretch in a jet-cooled, isolated dimer.[25]

Table 2 presents a simple Morse analysis of the experimental fundamental ($\tilde{\nu}_{N-H}$) and overtone ($2\tilde{\nu}_{N-H}$) values to provide anharmonicity constants $\omega_e x_e$ and harmonic wavenumbers ω_e based on

$$\omega_e x_e = \tilde{\nu}_{N-H} - \Delta\tilde{\nu}_{N-H}/2$$

and

$$\omega_e = \tilde{\nu}_{N-H} + 2\omega_e x_e$$

One should note that apart from a possible systematic error of the applied Morse analysis, the wavenumber uncertainties add for $\omega_e x_e$. Because of the low signal-to-noise ratio of the overtone band, we consider $\omega_e x_e$ to be accurate within 1–2 cm^{-1}. For ω_e itself, error propagation leads to an uncertainty of 3–4 cm^{-1}. It is seen that the harmonic dimer shifts obtained in this way agree even better with the B3LYP results[18] than the original anharmonic ones. However, before a definitive conclusion is drawn, overtone spectra with a better signal-to-noise ratio should be obtained, as combination transitions cannot be rigorously excluded as the origin of the D_d band. Furthermore, the disagreement between experiment and PW91 calculations becomes even worse upon inclusion of experimental anharmonicity.

In this context, a study of pyrrole in a liquid 1 : 1 mixture of CCl_3F and CF_2BrCF_2Br should be mentioned.[16] For the monomer, an anharmonic constant of 69 cm^{-1} was derived at room temperature from the overtone and fundamental positions, whereas the same analysis carried out for the main association band at lower temperature yielded a much increased value of 88 cm^{-1}. However, this corresponds to larger aggregates than dimers, as recognized by the authors. For the dimer itself, no anharmonicity estimate was derived.

A detailed but less critical analysis of CCl_4 solution data on pyrrole self-association has been presented recently.[17] Here, the N–H fundamental association band maximum was interpreted as being due to dimers, instead of larger aggregates. Since these larger aggregates do not absorb as strongly as dimers in the overtone region, a much too small donor anharmonicity constant of 27 cm^{-1} was derived for the pyrrole "dimer". The accompanying anharmonic B3LYP calculations[17] indeed nicely confirm our experimental finding that donor anharmonicity increases by about 10% upon dimer formation, rather than decreasing by 60%, as the experimental analysis in ref. 17 suggests. The fact that the donor fundamental wavenumber shift observed in CCl_4 solution is in apparently perfect agreement with our new dimer jet result (−86 cm^{-1}) is a consequence of error compensation: in CCl_4 at room temperature, the dimer is much less shifted relative to the monomer than in the low-temperature gas phase, as also evidenced by the overtone data.[17] However, the dominant aggregation species contributing to the fundamental spectrum is in fact a trimer or larger species,[16] whose enhanced red-shift compensates for the thermal weakening. This underscores that a correct interpretation of anharmonicity and hydrogen-bonding effects in pyrrole clusters requires low-temperature gas-phase experimental data, whereas solution data alone may lead to erroneous conclusions.

3.3 Dimers with pyrrole as a donor

To further explore the π–hydrogen bonding functionality of pyrrole, we have combined it with a range of acceptor molecules. By choosing molecules which are unable to act as N–H hydrogen-bond donors and by selecting low pyrrole concentrations, the resulting spectra are much simplified and easy to interpret. Nevertheless, stagnation pressure and relative concentrations were always varied to confirm the assignment of the mixed dimer peaks. Fig. 4 shows such a concentration series for the benzene–pyrrole system. At the lowest concentration of both compounds in He (trace c), only the pyrrole monomer and the heterodimer N–H stretching modes (D_{het}) remain visible. When both concentrations are increased (trace b), pure pyrrole aggregates (D_{hom}, T) start to appear and soon dominate the spectrum (trace a). This indicates that the hydrogen bonds between pyrrole molecules in the homodimer are stronger than those in the heterodimer between pyrrole and benzene. A more quantitative manifestation of this energy order can be found in the hydrogen-bond-

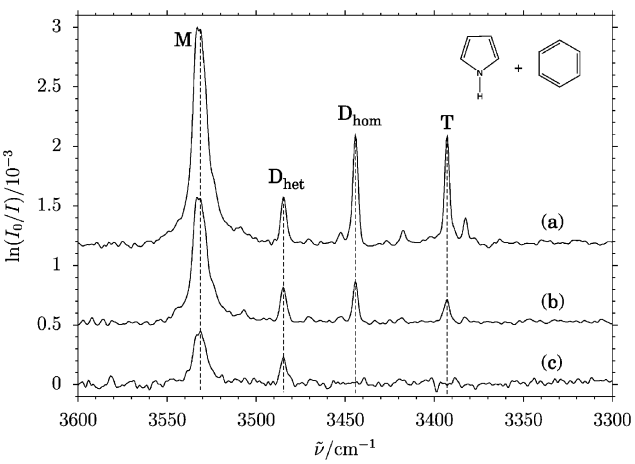

Fig. 4 Jet FTIR spectra of decreasing amounts of benzene and pyrrole co-expanded in He. (a) 0.04% pyrrole, 0.03% benzene, (b) 0.025% pyrrole, 0.03% benzene, (c) 0.02% pyrrole, 0.015% benzene. D_{het} marks signals from the pyrrole–benzene heterodimer and D_{hom} from the pyrrole homodimer.

 This journal is © the Owner Societies 2008

Published on 21 February 2008. Downloaded by Michigan State University on 23/01/2016 03:22:09.

induced red-shift. It is only 46 cm^{-1}, compared to 86 cm^{-1} in the pyrrole dimer. Since the donor and thus the IR probe molecule remains the same, this is an unequivocal proof for the stronger acceptor quality of pyrrole compared to benzene.[43] This is a well-known fact in solution chemistry, which may be related to the higher π-electron density, and which is here shown to be valid in the gas phase as well. Of course, detailed quantum-chemical calculations would be needed to substantiate such qualitative electron-density explanations, whereas the IR red-shift is a straightforward experimental variable. The complex of pyrrole with benzene has previously been investigated in CCl_4 solution[36] where the red-shift is only 30 cm^{-1} due to thermal weakening and competition by the solvent. The advantage of the gas-phase shift value of −46 cm^{-1} is that it allows for a direct comparison and judgement of quantum-chemical predictions.

In contrast to benzene, 1-methylpyrrole is expected to be a better hydrogen-bond acceptor than pyrrole itself, due to the electron-donating influence of the methyl group attached to the nitrogen. In perfect agreement with this expectation, the red-shift of the mixed dimer relative to pyrrole is now 93 cm^{-1}. There is evidence for larger clusters in the spectra at higher stagnation pressures, which require more systematic investigation. By further methylating the carbon atoms bound to nitrogen, the electron density of pyrrole can be further increased. As a consequence, the mixed dimer of pyrrole with 1,2,5-trimethylpyrrole absorbs 120 cm^{-1} lower in wavenumber than the pyrrole monomer, or 34 cm^{-1} lower than the pyrrole dimer.

3.4 Dimers with 2,5-dimethylpyrrole as a donor

To rule out accidental coincidences, we have carried out an analogous study for 2,5-dimethylpyrrole instead of pyrrole. Its self-aggregation spectrum is analogous to that of pyrrole. Relative to the monomer band at 3504 cm^{-1}, there are red-shifted cluster absorptions (Fig. 5b). Due to the reduced rotational constants, the dimer acceptor band is now better resolved on the slope of the monomer absorption and occurs 6 cm^{-1} to the red, similar to pyrrole. The dimer donor band has a shift of 84 cm^{-1}, close to the pyrrole dimer. The single IR-active trimer band occurs at a bathochromic shift of 132 cm^{-1}, slightly less than in the pyrrole trimer (138 cm^{-1}) but undoubtedly in a cyclic structure like pyrrole. The higher electron density is reflected in the lower monomer frequency value compared to pyrrole, but not in larger hydrogen-bond-induced red-shifts. The reason for this is that the better acceptor quality of 2,5-dimethylpyrrole is more than offset by the poorer donor quality of this electron-rich system. Steric hindrance due to the additional methyl groups may be another contributing aspect.

To separate the donor and acceptor influences, a series of acceptors was again studied in combination with the same donor (Fig. 5). Indeed, benzene now only induces a shift of −37 cm^{-1} in the heterodimer. The shift induced by 1-methylpyrrole is −61 cm^{-1}, while that induced by 1,2,5-trimethylpyrrole is −86 cm^{-1} and thus slightly larger than in the homodimer.

3.5 Correlation of dimer red-shift and acceptor quality

The observed regularities in the two series of dimers suggest a uniform correlation of acceptor quality and hydrogen-bond-induced red-shift in the gas phase, independent of the donor molecule. Fig. 6 contains such an attempt of ordering the gas-phase acceptors benzene, pyrrole, 1-methylpyrrole, 2,5-dimethylpyrrole and 1,2,5-trimethylpyrrole. They are ordered on the abscissa in such a way that the red-shifts which they

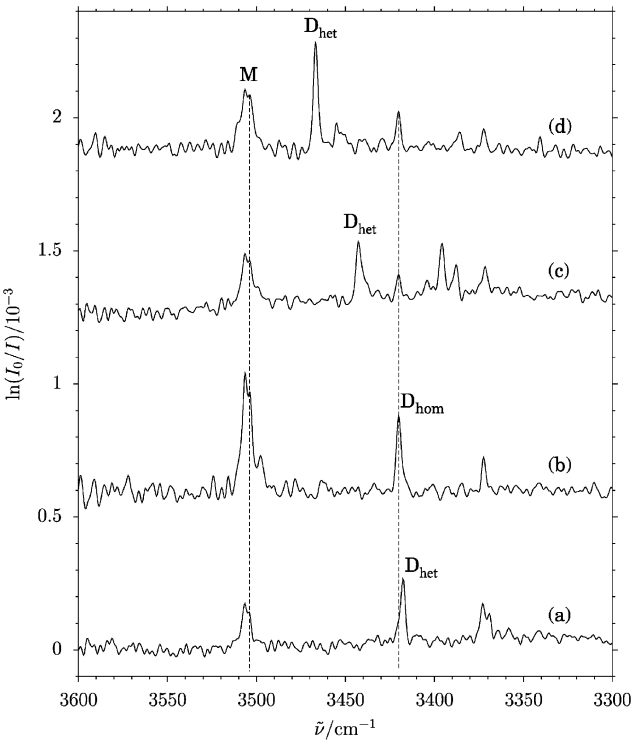

Fig. 5 Jet FTIR spectra of 2,5-dimethylpyrrole co-expanded with a range of acceptor molecules in He: (a) 1,2,5-trimethylpyrrole, (b) 2,5-dimethylpyrrole, (c) *N*-methylpyrrole, (d) benzene. D_{het} marks signals from the heterodimers and D_{hom} from the dimethylpyrrole homodimer.

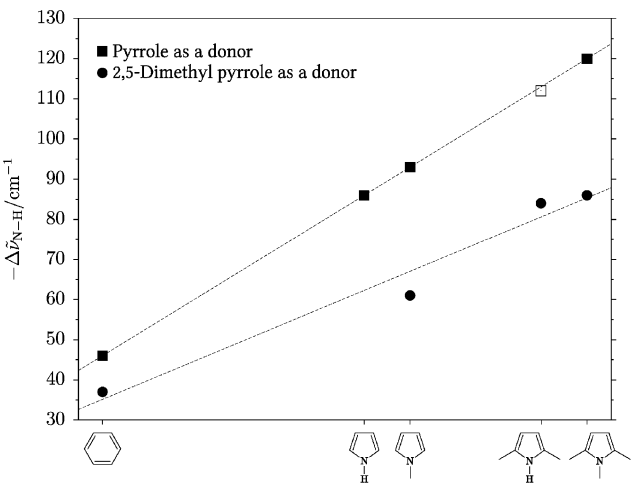

Fig. 6 Correlation between experimental N–H red-shifts and a postulated relative hydrogen-bond-acceptor quality for a range of π systems towards pyrrole (squares) and dimethylpyrrole (circles). The red-shift of dimethylpyrrole acting as an acceptor towards pyrrole (open square) is close to the prediction (upper dashed line), showing that the acceptor quality defined in this way is transferable among different donors. See text for further details.

Published on 21 February 2008. Downloaded by Michigan State University on 23/01/2016 03:22:09.

induce in pyrrole are represented by a straight line (upper dashed line connecting the filled squares). In the case of dimethylpyrrole, for which no mixed dimer with pyrrole as a donor was included, the same effect of *N*-methylation as in pyrrole was assumed in positioning it on the abscissa. While fixing this quantitative sequence of acceptor strengths derived from pyrrole, the shifts observed for dimethylpyrrole as a donor are included in the graph (filled circles roughly following the lower straight line). They are consistently smaller than those for pyrrole, reflecting the inferior donor quality and electronic properties of the N–H and possibly also the increased steric hindrance. Within the scattering and limited number of the dimethylpyrrole data points, their trend is found to be monotonous and therefore the acceptor-quality scale is seen to be transferable from that obtained with pyrrole. Hence, reasonably reliable predictions for the missing combinations are possible, *e.g.* the band positions of the two isomers of the mixed pyrrole–dimethylpyrrole dimer are predicted at 3418 (pyrrole as donor) and 3442 cm^{-1} (pyrrole as acceptor) respectively. The dimer in which pyrrole acts as a hydrogen-bond donor is predicted to be more stable. A recent measurement of this system reveals a single mixed dimer peak at 3419 cm^{-1} (open square), providing a nice confirmation of the correlation and energy sequence. The metastable dimer with inverted donor/acceptor roles is predicted close to the pyrrole dimer and falls below the noise level, *i.e.* it is at least an order of magnitude less abundant.

In summary, *C*-methylation of pyrroles is seen to have a larger effect on acceptor quality than *N*-methylation. Double *C*-methylation of pyrrole is found to have an effect similar to that of the switch from benzene to pyrrole. The acceptor sequence is transferrable between different donors and allows for accurate predictions of mixed pyrrole dimer absorptions.

4. Conclusions and outlook

Pyrrole is confirmed to form structurally well-defined hydrogen-bonded aggregates. Its bonds are confirmed to be somewhat weaker than those of classical hydrogen bonds such as those found in alcohols[13] or pyrazoles,[4] but stronger than those between simple amines,[16] based on vibrational red-shifts induced in the hydride stretching fundamentals.[44] Hydrogen bonding moderately increases the anharmonicity of the involved donor N–H bond by about 10%.

While density functionals can fail dramatically for clusters where there is an interplay between hydrogen-bond and dispersion forces,[45] the B3LYP method describes the spectra of pyrrole clusters quite satisfactorily.[18] Comparison to much poorer PW91 predictions suggests that the performance of B3LYP is likely to be coincidental and that inclusion of exact exchange into the functional is advisable. A more quantitative representation of the cluster spectra and energetics will require higher-level correlation treatments,[46,47] which the present experimental study on a particularly simple prototype wishes to encourage. The key question is: are pyrrole dimer calculations at a high level of electron correlation treatment capable of reproducing the experimental harmonic(!) monomer–dimer N–H stretching shift of -74 ± 4 cm^{-1}?

On the experimental side, the present contribution together with the recent work of Matsumoto and Honma[21] shows that FTIR, cavity ringdown and spontaneous Raman spectra are powerful and nicely complementary techniques when probing hydride stretching vibrations of hydrogen-bonded complexes. It would now be instructive to study lower-frequency modes in the jet-cooled clusters, notably the out-of-plane bending modes of pyrrole for which the matrix-isolation study[18] indicates interesting cluster shifts. Furthermore, mixed clusters involving more than two building blocks promise interesting hydrogen-bond topologies.

Acknowledgements

We thank the Fonds der Chemischen Industrie and the DFG (research training group 782 and project Su 121/2) for support. This study has profited from discussions with R. Fausto.

References

1 G. R. Desiraju and T. Steiner, *The Weak Hydrogen Bond in Structural Chemistry and Biology*, Oxford University Press, Oxford, 1999.
2 T. Steiner and G. Koellner, Hydrogen bonds with π-acceptors in proteins: frequencies and role in stabilizing local 3D structures, *J. Mol. Biol.*, 2001, **305**, 535–557.
3 C. Emmeluth, V. Dyczmons, T. Kinzel, P. Botschwina, M. A. Suhm and M. Yáñez, Combined jet relaxation and quantum-chemical study of the pairing preferences of ethanol, *Phys. Chem. Chem. Phys.*, 2005, **7**, 991–997.
4 C. A. Rice, N. Borho and M. A. Suhm, Dimerization of pyrazole in slit-jet expansions, *Z. Phys. Chem.*, 2005, **219**, 379–388.
5 K. Buchhold, B. Reimann, S. Djafari, H.-D. Barth, B. Brutschy, P. Tarakeshwar and K. S. Kim, Fluorobenzene and *p*-difluorobenzene microsolvated by methanol: an infrared spectroscopic and *ab initio* theoretical investigation, *J. Chem. Phys.*, 2000, **112**, 1844–1858.
6 T. Scharge, T. Häber and M. A. Suhm, Quantitative chirality synchronization in trifluoroethanol dimers, *Phys. Chem. Chem. Phys.*, 2006, **8**, 4664–4667.
7 E. A. Meyer, R. K. Castellano and F. Diederich, Interactions with aromatic rings in chemical and biological recognition, *Angew. Chem., Int. Ed.*, 2003, **42**, 1210–1250.
8 J. R. Carney, F. C. Hagemeister and T. S. Zwier, The hydrogen-bonding topologies of indole–$(water)_n$ clusters from resonant ion-dip infrared spectroscopy, *J. Chem. Phys.*, 1998, **108**, 3379–3382.
9 B. Küstner, C. Schmuck, P. Wich, C. Jehn, S. K. Srivastava and S. Schlücker, UV resonance Raman spectroscopic monitoring of supramolecular complex formation: peptide recognition in aqueous solution, *Phys. Chem. Chem. Phys.*, 2007, **9**, 4598–4603.
10 Y. Wang, H. Fu, A. Peng, Y. Zhao, J. Ma, Y. Ma and J. Yao, Distinct nanostructures from isomeric molecules of bis(iminopyrrole)benzenes: effects of molecular structures on nanostructural morphologies, *Chem. Commun.*, 2007, 1623–1625.
11 G. Columberg and A. Bauder, Pure rotational spectrum, quadrupole coupling constants and structure of the dimer of pyrrole, *J. Chem. Phys.*, 1997, **106**, 504–510.
12 M. Quack, U. Schmitt and M. A. Suhm, FTIR spectroscopy of hydrogen fluoride clusters in synchronously pulsed supersonic jets: isotopic isolation substitution and 3-d condensation, *Chem. Phys. Lett.*, 1997, **269**, 29–38.
13 T. Häber, U. Schmitt and M. A. Suhm, FTIR spectroscopy of molecular clusters in pulsed supersonic slit-jet expansions, *Phys. Chem. Chem. Phys.*, 1999, **1**, 5573–5582.
14 A. Mellouki, R. Georges, M. Herman, D. L. Snavely and S. Leytner, Spectroscopic investigation of ground state pyrrole ($^{12}C_4H_5N$): the N–H stretch, *Chem. Phys.*, 1997, **220**, 311–322.
15 C. Douketis and J. P. Reilly, The NH stretch in pyrrole: a study of the fundamental ($\Delta\nu = 1$) and third overtone ($\Delta\nu = 4$) bands in

 This journal is © the Owner Societies 2008

Published on 21 February 2008. Downloaded by Michigan State University on 23/01/2016 03:22:09.

the bulk gas and in a molecular beam, *J. Chem. Phys.*, 1992, **96**, 3431–3440.
16 M.-C. Bernard-Houplain and C. Sandorfy, Low-temperature infrared study of hydrogen bonding in dissolved pyrrole and indole, *Can. J. Chem.*, 1973, **51**, 1075–1082.
17 V. Stefov, L. Pejov and B. Soptrajanov, Experimental and quantum-chemical study of pyrrole self-association through N–H···π hydrogen bonding, *J. Mol. Struct.*, 2003, **651–653**, 793–805.
18 A. Gómez-Zavaglia and R. Fausto, Self-aggregation in pyrrole: matrix isolation, solid-state infrared spectroscopy and DFT study, *J. Phys. Chem. A*, 2004, **108**, 6953–6967.
19 V. Poterya, V. Profant, M. Fárník, P. Slavíček and U. Buck, Experimental and theoretical study of the pyrrole cluster photochemistry: closing the πσ* dissociation pathway by complexation, *J. Chem. Phys.*, 2007, **127**, 064307.
20 J. Wei, A. Kuczmann, J. Riedel, F. Renth and F. Temps, Photofragment velocity map imaging of H atom elimination in the first excited state of pyrrole, *Phys. Chem. Chem. Phys.*, 2003, **5**, 315–320.
21 Y. Matsumoto and K. Honma, NH stretching vibrations of pyrrole clusters studied by infrared cavity ringdown spectroscopy, *J. Chem. Phys.*, 2007, **127**, 184310.
22 V. Profant, V. Poterya, M. Fárník, P. Slavíček and U. Buck, Fragmentation dynamics of size-selected pyrrole clusters prepared by electron impact ionization forming a solvated dimer ion core, *J. Phys. Chem. A*, 2007, **111**, 12477–12486.
23 R. Kostic, S. A. Stepanyan, D. Rakovic, I. E. Davidova and L. A. Gribov, IR study of 1-methylpyrrole and 2,5-dimethylpyrrole, *J. Serb. Chem. Soc.*, 1994, **59**, 547–550.
24 C. Sándorfy, Hydrogen bonding: how much anharmonicity, *J. Mol. Struct.*, 2006, **790**, 50–54.
25 T. Scharge, D. Luckhaus and M. A. Suhm, Observation and quantification of the hydrogen bond effect on O–H overtone intensities in an alcohol dimer, *Chem. Phys.*, 2008, DOI: 10.1016/j.chemphys.2008.01.028.
26 N. Borho, M. A. Suhm, K. L. Barbu-Debus and A. Zehnacker, Intra- *vs.* intermolecular hydrogen bonding: dimers of alpha-hydroxyesters with methanol, *Phys. Chem. Chem. Phys.*, 2006, **8**, 4449–4460.
27 T. Nakanaga, F. Ito and H. Takeo, Time-resolved high-resolution FTIR absorption spectroscopy in a pulsed discharge, *Chem. Phys. Lett.*, 1993, **206**, 73–76.
28 T. Häber, U. Schmitt, C. Emmeluth and M. A. Suhm, Ragout-jet FTIR spectroscopy of cluster isomerism and cluster dynamics: from carboxylic acid dimers to N_2O nanoparticles, *Faraday Discuss.*, 2001, **118**, 331–359 and contributions to the discussion on pp. 53, 119, 174–175, 179–180, 304–309, 361–363, 367–370.
29 S. Hirabayashi and Y. Hirahara, Step-scan Fourier transform infrared absorption spectroscopy of acetylene monomer and solid in a supersonic free jet, *Chem. Phys. Lett.*, 2002, **361**, 265–270.
30 M. Herman, R. Georges, M. Hepp and D. Hurtmans, High-resolution Fourier transform spectroscopy of jet-cooled molecules, *Int. Rev. Phys. Chem.*, 2000, **19**, 277–325.
31 B. Maté, G. Tejada and S. Montero, Raman spectroscopy of supersonic jets of CO_2: density, condensation, and translational, rotational, and vibrational temperatures, *J. Chem. Phys.*, 1998, **108**, 2676–2685.
32 P. Zielke and M. A. Suhm, Concerted proton motion in hydrogen-bonded trimers: a spontaneous Raman scattering perspective, *Phys. Chem. Chem. Phys.*, 2006, **8**, 2826–2830.
33 M. J. Frisch, G. W. Trucks, H. B. Schlegel, G. E. Scuseria, M. A. Robb, J. R. Cheeseman, J. A. Montgomery, Jr., T. Vreven, K. N. Kudin, J. C. Burant, J. M. Millam, S. S. Iyengar, J. Tomasi, V. Barone, B. Mennucci, M. Cossi, G. Scalmani, N. Rega, G. A. Petersson, H. Nakatsuji, M. Hada, M. Ehara, K. Toyota, R. Fukuda, J. Hasegawa, M. Ishida, T. Nakajima, Y. Honda, O. Kitao, H. Nakai, M. Klene, X. Li, J. E. Knox, H. P. Hratchian, J. B. Cross, V. Bakken, C. Adamo, J. Jaramillo, R. Gomperts, R. E. Stratmann, O. Yazyev, A. J. Austin, R. Cammi, C. Pomelli, J. Ochterski, P. Y. Ayala, K. Morokuma, G. A. Voth, P. Salvador, J. J. Dannenberg, V. G. Zakrzewski, S. Dapprich, A. D. Daniels, M. C. Strain, O. Farkas, D. K. Malick, A. D. Rabuck, K. Raghavachari, J. B. Foresman, J. V. Ortiz, Q. Cui, A. G. Baboul, S. Clifford, J. Cioslowski, B. B. Stefanov, G. Liu, A. Liashenko, P. Piskorz, I. Komaromi, R. L. Martin, D. J. Fox, T. Keith, M. A. Al-Laham, C. Y. Peng, A. Nanayakkara, M. Challacombe, P. M. W. Gill, B. G. Johnson, W. Chen, M. W. Wong, C. Gonzalez and J. A. Pople, *GAUSSIAN 03 (Revision B.04)*, Gaussian, Inc., Wallingford, CT, 2004.
34 R. Wugt Larsen, P. Zielke and M. A. Suhm, Hydrogen-bonded OH stretching modes of methanol clusters: A combined IR and Raman isotopomer study, *J. Chem. Phys.*, 2007, **126**, 194307.
35 M. A. Martoprawiro and G. B. Bacskay, Quantum-chemical studies of the pyrrole–water and pyridine–water complexes, *Mol. Phys.*, 1995, **85**, 573–585.
36 M. S. Nozari and R. S. Drago, Spectral and Calometric Studies of Hydrogen Bonding with Pyrrole, *J. Am. Chem. Soc.*, 1970, **92**, 7086–7090.
37 H. Park and S. Lee, *Ab initio* investigations of the pyrrole dimer: a direct observation of the π-facial hydrogen bond, *Chem. Phys. Lett.*, 1999, **301**, 487–492.
38 T. Ebata, T. Watanabe and N. Mikami, Evidence for the cyclic form of phenol trimer: vibrational spectroscopy of the OH stretching vibrations of jet-cooled phenol dimer and trimer, *J. Phys. Chem.*, 1995, **99**, 5761–5764.
39 A. V. Bochenkova, M. A. Suhm, A. A. Granovsky and A. V. Nemukhin, Hybrid diatomics-in-molecules-based quantum-mechanical/molecular-mechanical approach applied to the modeling of structures and spectra of mixed molecular clusters $Ar_n(HCl)_m$ and $Ar_n(HF)_m$, *J. Chem. Phys.*, 2004, **120**, 3732–3743.
40 N. Borho and M. A. Suhm, Glycidol dimer: anatomy of a molecular handshake, *Phys. Chem. Chem. Phys.*, 2002, **4**, 2721–2732.
41 T. Di Paolo, C. Bourdéron and C. Sandorfy, Model calculations on the influence of mechanical and electrical anharmonicity on infrared intensities: relation to hydrogen bonding, *Can. J. Chem.*, 1972, **50**, 3161–3166.
42 A. Mellouki, J. Liévin and M. Herman, The vibrational spectrum of pyrrole (C_4H_5N) and furan (C_4H_4O) in the gas phase, *Chem. Phys.*, 2001, **271**, 239–266.
43 C. Emmeluth, V. Dyczmons and M. A. Suhm, Tuning the hydrogen bond donor/acceptor isomerism in jet-cooled mixed dimers of aliphatic alcohols, *J. Phys. Chem. A*, 2006, **110**, 2906–2915.
44 A. V. Iogansen, Direct proportionality of the hydrogen bonding energy and the intensification of the stretching ν(XH) vibration in infrared spectra, *Spectrochim. Acta, Part A*, 1999, **55**, 1585–1612.
45 T. B. Adler, N. Borho, M. Reiher and M. A. Suhm, Chirality-induced switch in hydrogen-bond topology: tetrameric methyl lactate clusters in the gas phase, *Angew. Chem., Int. Ed.*, 2006, **45**, 3440–3445.
46 A. Tekin and G. Jansen, How accurate is the density functional theory combined with symmetry-adapted perturbation theory approach for CH–π and π–π interactions? A comparison to supermolecular calculations for the acetylene–benzene dimmer, *Phys. Chem. Chem. Phys.*, 2007, **9**, 1680–1687.
47 J. Černý and P. Hobza, Non-covalent interactions in biomacromolecules, *Phys. Chem. Chem. Phys.*, 2007, **9**, 5291–5303.